

Learning to Advise and Learning from Advice in Cooperative Multi-Agent Reinforcement Learning

Yue Jin¹, Shuangqing Wei², Jian Yuan¹, Xudong Zhang¹

¹ Department of Electronic Engineering, Tsinghua University, Beijing, China

² School of Electrical Engineering and Computer Science, Louisiana State University, Baton Rouge, USA
 jiny23@126.com, swei@lsu.edu, jyuan@tsinghua.edu.cn, zhangxd@tsinghua.edu.cn

Abstract—Learning to coordinate is a daunting problem in multi-agent reinforcement learning (MARL). Previous works have explored it from many facets, including cognition between agents, credit assignment, communication, expert demonstration, etc. However, less attention were paid to agents’ decision structure and the hierarchy of coordination. In this paper, we explore the spatiotemporal structure of agents’ decisions and consider the hierarchy of coordination from the perspective of multilevel emergence dynamics, based on which a novel approach, Learning to Advise and Learning from Advice (LALA), is proposed to improve MARL. Specifically, by distinguishing the hierarchy of coordination, we propose to enhance decision coordination at meso level with an advisor and leverage a policy discriminator to advise agents’ learning at micro level. The advisor learns to aggregate decision information in both spatial and temporal domains and generates coordinated decisions by employing a spatiotemporal dual graph convolutional neural network with a task-oriented objective function. Each agent learns from the advice via a policy generative adversarial learning method where a discriminator distinguishes between the policies of the agent and the advisor and boosts both of them based on its judgement. Experimental results indicate the advantage of LALA over baseline approaches in terms of both learning efficiency and coordination capability. Coordination mechanism is investigated from the perspective of multilevel emergence dynamics and mutual information point of view, which provides a novel perspective and method to analyze and improve MARL algorithms.

Index Terms—multi-agent reinforcement learning, coordination, graph neural network, generative adversarial network, multi-level emergence dynamics, mutual information

I. INTRODUCTION

The emergence of collective intelligence is a fascinating topic. People are intrigued by creating collective artificial intelligence. Deep multi-agent reinforcement learning (MARL) is one of the inspiring achievements in cooperative agents [1]–[5] in recent years. However, learning to coordinate is still a daunting problem in MARL.

Many facets have been explored to propel the emergence of coordination and accelerate learning. Learning cognition between agents is a natural idea when it comes to coordination. Fruitful investigation have been conducted along this direction [6]–[8]. Credit assignment [9]–[12] is another critical exploration, whose goal is to learn individual credit in the settings with a sharing reward function. Another branch of studies proposed to learn from experts. A typical class of methods is imitation learning, where agents learn from expert demonstrations [13]–[17]. However, the coordination mechanism is either not investigated or just explored from

the perspective of cognition between two agents in these methods. Communication provides a means of coordinating in a larger range and thereby facilitates coordination. Plenty of studies have been conducted to learn communication content [18], [19], choose communication agents [20], [21] and decide when to communicate [22]. Essentially, they involve information sharing mechanism, but seldom consider decision structure. Recently, some works [23], [24] have paid attention to decision execution structure, where agents make decisions based on a learned coordination graph reflecting their decision dependency. However, the intrinsic spatiotemporal structure of agents’ decisions have not been explored. In addition, these works mentioned above barely involve mutual interactions among agents’ decisions.

In this paper, we explore the spatiotemporal structure of agents’ decisions and the hierarchy of coordination, and propose a novel algorithm of Learning to Advise and Learning from Advice (LALA) to guide agents’ learning in cooperative MARL. Specifically, we consider the hierarchy of coordination from the perspective of multilevel emergence dynamics (MED) [25]–[28], where meso-level interaction plays a vital role in the emergence process of coordination. Therefore, we propose to enhance decision interplay at meso level via a centralized advisor who leverages the spatiotemporal decision structure of agents to coordinate decisions. Micro-level agents are guided by the advisor on policy learning in addition to their own exploration. We focus on cooperative multi-agent tasks where agents need to avoid decision conflicts, such as cooperative navigation tasks [7], [8], [29], [30] (shown as Fig. 1) where agents need to select different targets and minimize the overall navigation time, and multi-arm robot control tasks [31]–[33] involving position conflicts. Coordination includes resolving decision conflicts and smoothing decisions in these tasks.

Specifically, we employ a spatiotemporal graph to characterize the relations between agents’ decisions in both spatial and temporal domains. We propose a spatiotemporal dual graph neural network (DualGCN) to aggregate agents’ decision information and generate coordinated decision advice. The DualGCN takes the graph structure and agents’ decisions as inputs, and mitigates decision conflicts and discontinuity by distinguishing and clustering decision features of different agents and different time steps, respectively.

A policy-level generative adversarial network (PLGAN) is proposed for agents to learn from the advice. It includes a discriminator that distinguishes between the policies of

the agent and the advisor. The discriminator's judgement is utilized to guide agent's policy learning and boost the coordination capability of DualGCN. Agent's decision network adopts an information bottleneck [34] based encoder for low-dimensional representation and compression of observations. The learned latent variables are used to infer other agents' actions, and taken as inputs of agent's decision network. Note that, LALA is developed to help learn to coordinate. Once learned, only the decision network is deployed onto each agent to complete tasks.

We investigate the efficacy and advantage of LALA from multilevel system perspective and mutual information point of view. Specifically, mutual information gain between agent's local observation and other agents' decisions is utilized to examine the cognition between agents at micro level. At meso level, we verify the coordination improvement caused by the decision interaction of DualGCN. Bridging different levels, we investigate if the advice generated from meso-level decision interaction affects the cognition between micro-level agents, and examine how the micro-level cognition and meso-level interaction affect macro-level coordination performance.

The main contributions of this paper are as follows.

- A LALA approach is proposed to improve MARL and propel coordination, which coordinates agents' decisions based on their spatiotemporal structure and guides agents' learning with the coordinated decision advice.
- We investigate coordination mechanism from the perspective of multilevel emergence dynamics and mutual information point of view, which provides a novel perspective and method to analyze and improve MARL algorithms.
- Extensive experimental results demonstrate the advantage of LALA over baseline MARL algorithms in terms of both learning efficiency and cooperation performance.

II. PROBLEM FORMULATION

We consider a Stochastic Game (SG) with N agents, which involves state s , joint action $\mathbf{a} = (a_1, \dots, a_N)$, transition probability function $p(s'|s, \mathbf{a})$, and reward function $r_i(s, \mathbf{a}), i \in \{1, \dots, N\}$. At each time step, each agent executes an action according to its policy π_i which maps the state to an action probability. Let $\boldsymbol{\pi} = (\pi_1, \dots, \pi_N)$ denote the joint policy.

In this work, we focus on solving a kind of fully cooperative tasks where 1) the policy of each agent is stochastic and with discrete action space; 2) a decision conflict emerges when two agents choose the same action. Formally, $a_i \in \{c_z\}_{z=1}^Z$, where Z is the size of the action set, c_z is the z -th element of the action set. The policy of each agent satisfies $\forall z, \pi_i(a_i = c_z|s) \in [0, 1]$, and $\sum_{z=1}^Z \pi_i(a_i = c_z|s) = 1$. When $\arg \max_{c_z} \pi_i(a_i = c_z|s) = \arg \max_{c_z} \pi_j(a_j = c_z|s)$, a conflict occurs, and all the agents cannot get maximal reward.

The goal is to find the optimal policy for each agent so that $\forall \pi_i, R_i(s^t, \pi_1^*, \dots, \pi_i^*, \dots, \pi_N^*) \geq R_i(s^t, \pi_1^*, \dots, \pi_i, \dots, \pi_N^*)$, where π_i^* denotes the optimal policy of agent i , and $R_i(s^t, \boldsymbol{\pi}) = E[\sum_{\tau=0}^T \gamma^\tau r_i(s^{t+\tau}, \mathbf{a}^{t+\tau})]$ denotes the expectation of its cumulative discounted reward.

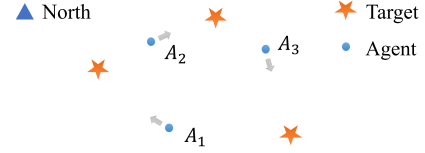


Fig. 1: An illustration of cooperative navigation.

III. PRELIMINARIES

In this section, we present some preliminary knowledge, including background about MARL and an algorithm used as a baseline in our experiments; background about GCN and a general model; multi-agent imitation learning with GAN and a typical algorithm involved in our baseline methods.

A. MARL

The optimal policy of an SG with unknown transition probability and reward function can be solved by MARL. An individual Q-function [2], [35] is defined as follows:

$$Q_i(s, a_i) = \mathbb{E}[\sum_{\tau} \gamma^\tau r_i^{t+\tau} | s^t = s, a_i^t = a_i]. \quad (1)$$

It measures the expected total discounted rewards of agent i who takes action a_i in state s and following π_i thereafter. An extended action-value function is proposed to take other agents' actions into consideration [2], which is defined as $Q_i^{\pi_i}(s^t, \zeta(s_{-i}^t, s_{-i}^{t+1}), a_i^t)$. ζ is an estimation function of other agents' actions, s_{-i} is the part of state regarding other agents. An approximate Bellman equation for the optimal extended Q-function is derived as:

$$\begin{aligned} \mathbb{E}_{s_{-i}^{t+1}} Q_i^*(s^t, \zeta(s_{-i}^t, s_{-i}^{t+1}), a_i^t) &\approx \\ \mathbb{E}_{s_{-i}^{t+1}} [r_i^{t+1} + \gamma \max_{a_i^{t+1}} Q_i^*(s^{t+1}, \zeta(s_{-i}^t, s_{-i}^{t+1}), a_i^{t+1})], \end{aligned} \quad (2)$$

Based on [2], IBORM algorithm [8] leverages information bottleneck principle to compress the input information of action estimation, while retaining the information regarding other agents' actions. The network architecture of IBORM is shown in Fig. 2. The loss function for the extended Q-function is given as:

$$\begin{aligned} \mathcal{L}_i^{\theta_i} &= \mathbb{E} \left[\left(y_i^t - Q_i^{\theta_i}(s^t, \eta(\phi_{-i,1}^{t+1}), \dots, \eta(\phi_{-i,N-1}^{t+1}), a_i^t) \right)^2 \right] \\ &+ \sum_{j=1}^{N-1} [\rho_1 \cdot \mathcal{L}_{CE}(\hat{a}_{-i,j}^t; a_{-i,j}^t) + \rho_2 \cdot I(\phi_{-i,j}^{t+1}; \eta(\phi_{-i,j}^{t+1})) \\ &- \rho_3 \cdot I(\eta(\phi_{-i,j}^{t+1}); a_{-i,j}^t)], \end{aligned} \quad (3)$$

where θ_i is parameters of the extended Q-function; $\phi_{-i,j}^{t+1} = (s_{-i,j}^t, s_{-i,j}^{t+1})$ denotes the states of the j -th agent except agent i at two adjacent time steps; η is an encoder to extract the representation relevant to the action of an agent; \mathcal{L}_{CE} denotes the cross entropy between the estimated action $\hat{a}_{-i,j}^t = \kappa(\eta(\phi_{-i,j}^t))$ and the true action $a_{-i,j}^t$; κ is a function that maps the action representation to the estimated action; I denotes mutual information; and $y_i^t = r_i^{t+1} + \gamma \max_{a_i^{t+1}} Q_i^{\theta_i}(s^{t+1}, \eta(\phi_{-i,1}^{t+1}), \dots, \eta(\phi_{-i,N-1}^{t+1}), a_i^{t+1})$. Based on the two mutual information terms, IBORM learns optimal

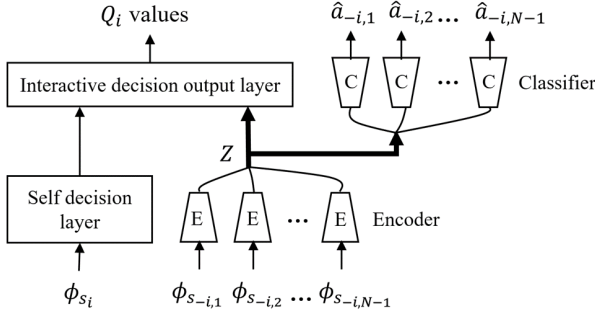


Fig. 2: Network architecture diagram of IBORM [8].

representations of other agents' actions and thus helps learn coordinated policies more efficiently.

B. GCN

Graph is an effective tool to represent the relationships between entities in a system, which has been used to represent physical systems [36], social networks [37], road networks [38], protein interaction networks [39], etc. We denote a graph as $\mathcal{G} = (\mathcal{V}, \mathcal{E})$, where \mathcal{V} is a set of vertices, and \mathcal{E} is a set of edges. Let $e_{uv} = (u, v)$ denote an edge connecting vertex u and vertex v . The set of neighbors of vertex v is denoted as $\mathcal{N}(v) = \{u | (u, v) \in \mathcal{E}\}$.

Based on the graph structure and leveraging convolution operators, a GCN can aggregate information within neighborhoods [40], [41]. As multiple graph convolutional layers are stacked, neighbors within multiple skips can be involved in information aggregation. A GCN takes the original features of each vertex and the graph structure as input, and can output features for each vertex, each edge, or the overall graph according to the need of a task, such as node classification [42], link prediction [43], or graph classification [44], respectively.

GraphSAGE [42] was proposed as a general aggregation-based graph convolution model. In the k -th convolutional layer, features are aggregated as:

$$\begin{aligned} \mathbf{h}_{\mathcal{N}_v}^k &= \text{AGG}_k(\{\mathbf{h}_u^{k-1}, \forall u \in \mathcal{N}(v)\}) \\ \mathbf{h}_v^k &= \varphi(g^k([\mathbf{h}_v^{k-1}, \mathbf{h}_{\mathcal{N}_v}^k])), \end{aligned} \quad (4)$$

where AGG_k denotes an aggregation function, e.g., mean or max-pooling function; \mathbf{h}_v^k denotes the features of vertex v output by the k -th hidden layer; $[\cdot, \cdot]$ denotes concatenated vectors; g^k denotes a linear function, and φ denotes a nonlinear activation function. Specifically, in each convolutional layer, GraphSAGE first aggregates features of the neighbors for each vertex using an aggregation function. Then, it concatenates the aggregated neighbors' features with the vertex's own features, and uses the concatenated features to compute the output features of this vertex.

C. GAN in Multi-Agent Imitation Learning

A branch of studies in imitation learning leverages GAN to match the data distribution of the learned policy with the distribution of the expert demonstration data. Some works [13]–[15] have employed this idea in multi-agent imitation

learning. Typically, MAGAIL [13] solves policies by optimizing the following objective:

$$\begin{aligned} \min_{\pi} \max_{D_1, \dots, D_N} \mathbb{E}_{\pi} \left[\sum_{i=1}^N \log D_i(s, a_i) \right] \\ + \mathbb{E}_{\pi^E} \left[\sum_{i=1}^N \log(1 - D_i(s, a_i)) \right], \end{aligned} \quad (5)$$

where D_i denotes discriminator, $\pi^E = (\pi_1^E, \dots, \pi_N^E)$ denotes the experts' policies. Each discriminator maps state-action pairs to judging probabilities and thereby distinguishes between state-action pairs collected by agent's policy and the expert demonstrations. The policy of each agent plays the role of generator who fools the discriminator by matching its state-action distribution with that of the expert demonstration data.

IV. METHOD

In this section, we propose our proposed LALA method through the lens of MED. MED is a concept regarding a dynamic process of a system from micro-level individual behaviors and meso-level interplay, to macro-level emergence [25]–[28]. From the perspective of MED, we consider a cooperative multi-agent system as follows: (1) the micro-level behaviors lie in each agent's decision making; (2) the meso-level interplay corresponds to information interaction and decision coordination among agents; (3) the macro-level emergence is reflected by the success of completing a cooperation task. As an intermediate process, the meso-level interplay plays an important role in the emergence of coordination. Therefore, we propose LALA to enhance the meso-level decision interplay beyond micro agent scope with a centralized advisor module, and guide agents' learning at micro level.

Fig. 3 shows an overall illustration for LALA. At micro level, each agent makes decisions based on its local observations, and receives reward from the world. At meso level, a centralized advisor learns to coordinate agents' decisions based on agents' decisions and the spatiotemporal structure. At macro level, a discriminator learns to distinguish between the policies of an agent and the advisor. Based on discriminator's judgement, each agent learns to match with the advised policy, and the advisor learns to boost its advising capability. The framework is identical to each agent. Fig. 3 just takes one agent as an example. Blue arrows indicate the inter-level information flow.

Next, we first present the advisor (Section IV-A), followed by the MARL agents and discriminators (Section IV-B), and then an advisor boosting method (Section IV-C) based on the discriminators.

A. Meso-Level: Learning to Advise with DualGCN

At meso level, an example including two agents is shown in the bottom right part of Fig. 3. We leverage a spatiotemporal graph to characterize the relations between agents' decisions. Thus, the input feature of each vertex is the decision made by an agent at a time step. In this work, we focus on the fully cooperative tasks where agents need to avoid decision conflicts with each other, such as avoiding target selection

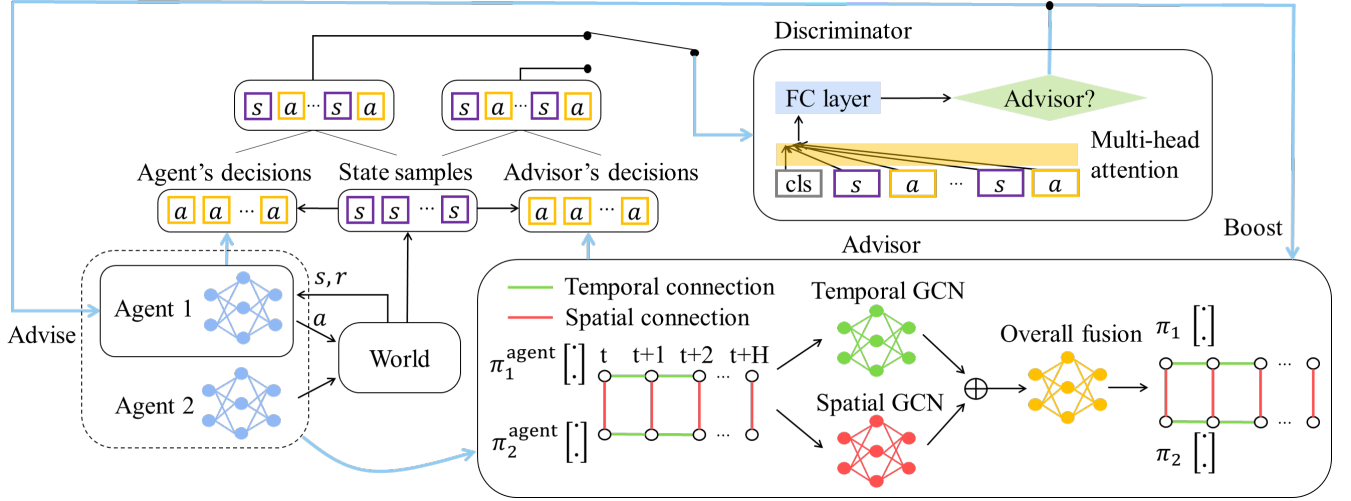


Fig. 3: Illustration of LALA framework. The bottom left part represents MARL agents who interact with the environment. The bottom right part illustrates DualGCN advisor whose input is a spatiotemporal graph including decisions of all agents. The upper part is a discriminator distinguishing between the state-action sets of the advisor and the agent. The discriminator provides guidance to boost the policies of both the MARL agents and the advisor.

conflicts in cooperative navigation tasks. To reflect the potential conflict between each two agents, vertices of different agents at the same time step are connected with each other in spatial dimension (red edges). Additionally, considering time continuity required in many control problems, i.e. the decisions at each two adjacent time steps need to be similar, we connect the vertices of the same agents along time dimension (green edges). Through the lens of the spatiotemporal graph, the advisor can view the decisions of each agent over the whole system and multiple time slots including the future, and thus generate better decisions to advise agents.

To generate advice, we propose a spatiotemporal dual GCN (DualGCN), where spatial conflicts and temporal discontinuity are mitigated via decision interaction at meso level. Specifically, to cope with constraints imposed on agents' decisions for maintaining temporal continuity and resolving spatial conflicts, the neighbors of each vertex are divided into two sets, $\mathcal{N}_s(v)$ and $\mathcal{N}_t(v)$. DualGCN fuses decision information within K -hop spatial and temporal neighborhoods in different manners (weights) and then fuses the overall spatiotemporal information to generate decision advice. An abstract illustration is shown in the bottom right part of Fig. 3.

Formally, in the k -th hidden layer, features are aggregated as follows:

$$\begin{aligned}
 \mathbf{m}_s^k &= \text{AGG}_k^s(\{\mathbf{h}_w^{k-1}, \forall w \in \mathcal{N}_s(v)\}) \\
 \mathbf{m}_t^k &= \text{AGG}_k^t(\{\mathbf{h}_u^{k-1}, \forall u \in \mathcal{N}_t(v)\}) \\
 \mathbf{h}_{\mathcal{N}_v}^k &= f^k([\mathbf{m}_s^k, \mathbf{m}_t^k]) \\
 \mathbf{h}_v^k &= \varphi(g^k([\mathbf{h}_v^{k-1}, \mathbf{h}_{\mathcal{N}_v}^k])),
 \end{aligned} \tag{6}$$

where AGG_k^s and AGG_k^t denote spatial and temporal aggregation function, respectively; \mathbf{h}_v^k is the features of vertex v output by the k -th hidden layer; $[\cdot, \cdot]$ denotes concatenating; f^k and g^k are linear functions to be learned; φ is a nonlinear activation function. The number of hidden layers determines how many hops of neighbors each vertex can interact with. The

more hidden layers the DualGCN has, the larger the scope of meso-level decision interactions is. The aggregating method is similar to GraphSAGE [42]. However, our method considers two types of neighbors, which is not involved in GraphSAGE.

The objective function for DualGCN is designed to mitigate spatial conflicts and temporal discontinuity by distinguishing and clustering the decisions belonging to different agents and time steps, respectively. Specifically, the goal is to lead the outputs of the vertices adjacent in temporal domain to be similar, and in spatial domain to be distinct. Therefore, we design a cost function consisting of temporal discontinuity cost and spatial conflict cost by measuring the decision similarity, shown as the first two terms in (8).

Additionally, as a conflict reconciler, the advisor needs to decide which agents should concede and which ones should not. To generate advice that can improve agents in a gradual manner, the advisor investigates the decision confidence of each agent, and corresponds its decision with the most confident one. To this end, we design a max-confidence consistency cost which measures the decision distance between the of the advisor and the most confident agent with Jensen-Shannon divergence. An indicator function expressing whether the decision is the most confident is given as:

$$I_{\text{label}}(v) = \begin{cases} 1, & \text{if } \forall w \in \mathcal{N}_s(v) \\ & \max_a \pi_v^{\text{agent}}(a) > \pi_w^{\text{agent}}(\arg \max_a \pi_v^{\text{agent}}(a)), \\ 0, & \text{otherwise} \end{cases} \tag{7}$$

where $\arg \max_a \pi_v^{\text{agent}}(a)$ is the preferred action of the agent represented by vertex v , and $\max_a \pi_v^{\text{agent}}(a)$ is the corresponding decision probability. As decision probability reflects decision confidence, (7) means that if the preferred action of an agent has the highest possibility among all agents' possibilities on this action, the decision is the most confident.

Algorithm 1: Learning to Advise with DualGCN

Input: Graph $\mathcal{G}(\mathcal{V}, \mathcal{E})$; vertex features $\{\pi_v^{\text{agent}}, \forall v \in \mathcal{V}\}$; state set \mathcal{B}_i^s , vertex set \mathcal{B}_i^v , depth K , training epoch number E

- 1 **Initialize:** Spatial weight matrices Ω_k^s , temporal weight matrices Ω_k^t , overall fusion weight matrices Ω_k^o , $k \in \{1, \dots, K\}$;
- 2 $\mathbf{h}_v^0 \leftarrow \pi_v^{\text{agent}}, \forall v \in \mathcal{V}$;
- 3 **for** $epoch = 1 \dots E$ **do**
- 4 **for** $k = 1 \dots K$ **do**
- 5 **for** $v \in \mathcal{V}$ **do**
- 6 Compute: $\mathbf{h}_{\mathcal{N}_v}^k = \Omega_k^s \cdot \text{AGG}_k^s(\{\mathbf{h}_w^{k-1}, \forall w \in \mathcal{N}_s(v)\}) + \Omega_k^t \cdot \text{AGG}_k^t(\{\mathbf{h}_u^{k-1}, \forall u \in \mathcal{N}_t(v)\})$
and $\mathbf{h}_v^k = \varphi(\Omega_k^o \cdot \text{CONCAT}(\mathbf{h}_v^{k-1}, \mathbf{h}_{\mathcal{N}_v}^k))$;
- 7 **end**
- 8 **end**
- 9 $\pi_v \leftarrow \text{Softmax}(\mathbf{h}_v^K), \forall v \in \mathcal{V}$;
- 10 Update $\Omega_k^s, \Omega_k^t, \Omega_k^o, k \in \{1, \dots, K\}$ to minimize (8) or (11);
- 11 **end**

The overall cost function of DualGCN advisor is given as:

$$\mathcal{L}_{Advisor} = \sum_{v \in \mathcal{V}} \left[\sum_{u \in \mathcal{N}_t(v)} -\log(\sigma(\pi_v^T \pi_u)) - \sum_{w \in \mathcal{N}_s(v)} \log(\sigma(-\pi_v^T \pi_w)) + I_{label}(v) \cdot JSD(\pi_v || \pi_v^{\text{agent}}) \right]. \quad (8)$$

where σ is the sigmoid function; the first two terms correspond to temporal discontinuity cost and spatial conflict cost; the last term corresponds to the max-confidence consistency cost.

The complete algorithm of learning to advise with DualGCN is shown in Algorithm 1.

B. Micro-Level: Learning from Advice with PLGAN

To bridge the information flow between the meso-level DualGCN advisor and micro-level agent's decision network, we propose a macro-level discriminator to distinguish between the advisor and agent policies and help boost them, which is illustrated as the upper part of Fig. 3.

To learn from the policy behind the advisor's advice given in the situations encountered by agents, we leverage a policy representation approach analogous to a recent work [45] to learn features of a policy from a set of states and the actions taken by the policy. The discriminator distinguishes between the agent and advisor based on the policy features.

Specifically, the discriminator consists of a Transformer encoder and a classifier. The Transformer encoder takes a set of state-action pairs that is structured as a sequence as raw input. A class token (CLS) [46] is concatenated with the raw input. The learned embedding of the CLS token is deemed the representation of the policy and then mapped by the classifier to a judging probability. Let $\mathcal{B}_i^s, \mathcal{A}_i^\pi$, and \mathcal{A}_i^G denote a set of states, actions mapped by the agent's

policy, and the advised actions given by the DualGCN advisor, respectively. \mathcal{D}^{ψ_i} denotes the discriminator parameterized with ψ_i . The loss function for the discriminator is defined as:

$$\mathcal{L}_{Disc,i} = -\mathbb{E}_{\mathcal{B}_i^s} [\log D^{\psi_i}(\mathcal{A}_i^G(\Omega), \mathcal{B}_i^s) + \log(1 - D^{\psi_i}(\mathcal{A}_i^\pi(\theta_i), \mathcal{B}_i^s))], \quad (9)$$

where Ω denotes parameters of DualGCN, and θ_i denotes parameters of the policy of agent i . Note that, the advisor is learned in a centralized manner and provides decision advice for all of the agents. Therefore, Ω is shared by all agents.

At micro level, each agent leverages the corresponding discriminator's judgement to match with the advisor's policy. Specifically, each agent learns to fool the discriminator, i.e. maximize the cost function (9), in addition to learning by its own exploration. The loss function for each agent is defined as:

$$\mathcal{L}_{Agent,i} = \mathcal{L}_i^{\theta_i} + \lambda \mathbb{E}_{\mathcal{B}_i^s} \log(1 - D^{\psi_i}(\mathcal{A}_i^\pi(\theta_i), \mathcal{B}_i^s)), \quad (10)$$

where $\mathcal{L}_i^{\theta_i}$ is the loss function for policy learning of an MARL algorithm and λ is a positive weight that balances agent's active learning and learning from advice. Note that, our method is different from imitation learning where reward signal is not available. We focus on the case where agents can receive environmental rewards and leverage the advice to improve learning.

The optimal loss corresponding to (9) is the Jensen-Shannon divergence between the state-action sets (policy features) of the agent and the advisor. By minimizing (9) and (10), each agent finds a policy under the constraint of matching its policy with the advised policy. Because the advised policy is coordinated and smoothed, agents can be guided to coordinate.

C. Meso-Level Boosting via Macro-Level Discriminator

In Section IV-A, we leverage DualGCN to reconcile decision conflicts and smooth decisions from a global spatiotemporal view, and thereby generate better decisions to advise the MARL. Intuitively, when we have two policies and know which is better, we can further boost the better one by exploiting strengths and avoiding weaknesses. Based on this idea, in this part, we propose to boost the advisor.

Actually, trained with (9), the discriminator presented in Section IV-B can give a higher probability score to the advisor than an agent. This probability score can thus be deemed a metric measuring the extent of advantage that the advisor's policy has over that of an agent. Therefore, the discriminator plays the role of an advantage function, which can be employed to boost the performance of the advisor's policy. We introduce an additional term into the original loss (8) of DualGCN, which reflects the advantage of the advisor's

Algorithm 2: LALA in MARL

```

1 Initialize: Parameters  $\Omega$  for GCN  $G^\Omega$ ; parameters  $\theta_i$ 
   for policy  $\pi^{\theta_i}$  and  $\psi_i$  for discriminator  $D^{\psi_i}$  of each
   agent; state buffer  $\mathcal{D}_i^s$  of each agent; overall decision
   buffer  $\mathcal{D}_\pi$ ; graph buffer  $\mathcal{G}$ ;
2 for  $episode = 1$  to  $C$  do
3   Receive  $s_i^1$  for each agent;
4   for  $t = 1$  to  $T$  do
5     for  $i = 1$  to  $N$  do
6       Execute action  $a_i^t \sim \pi^{\theta_i}(\cdot|s_i^t)$ ;
7       Record state  $\mathcal{D}_i^s \leftarrow \mathcal{D}_i^s \cup s_i^t$ ;
8       Record decision  $\mathcal{D}_\pi \leftarrow \mathcal{D}_\pi \cup \pi^{\theta_i}(\cdot|s_i^t)$ ;
9       if  $|\mathcal{D}_i^s| > \xi$  then
10        Sample state subset  $\mathcal{B}_i^s = \{s_i^{\tau_m}\}_{m=1}^M$ 
           from  $\mathcal{D}_i^s$  and record vertex index
            $\mathcal{B}_i^v = \{v_i^{\tau_m}\}_{m=1}^M$ ;
11        Compute decisions
            $\mathcal{A}_i^\pi = \{\pi^{\theta_i}(\cdot|s_i), \forall s_i \in \mathcal{B}_i^s\}$ ;
12        Compute advice
            $\mathcal{A}_i^G = \{G^\Omega(v_i), \forall v_i \in \mathcal{B}_i^v\}$ ;
13        Update  $\psi_i$  to minimize (9);
14      end
15    end
16    Receive  $r_i^{t+1}, s_i^{t+1}$  for each agent  $i$ ;
17    for  $i = 1$  to  $N$  do
18      Update  $\theta_i$  to minimize (10) with  $\mathcal{B}_i^s$ ;
19    end
20  end
21  Construct a spatiotemporal graph  $g$  with all agents'
   decisions made in the last episode;
22  Record graph  $\mathcal{G} \leftarrow \mathcal{G} \cup g$ ;
23  for  $i = 1$  to  $N$  do
24    Sample state subset  $\mathcal{B}_i^s = \{s_i^{\tau_m}\}_{m=1}^M$  from  $\mathcal{D}_i^s$ 
   and record vertex index  $\mathcal{B}_i^v = \{v_i^{\tau_m}\}_{m=1}^M$ ;
25  end
26  Update  $\Omega$  using Algorithm 1 with  $\mathcal{G}, \mathcal{D}_\pi, \{\mathcal{B}_i^s\}_{i=1}^N, \{\mathcal{B}_i^v\}_{i=1}^N$ ;
27 end

```

policy. Thus, the loss function for the advisor is given as:

$$\begin{aligned}
\mathcal{L}_{Advisor,boost} = & \sum_{v \in \mathcal{V}} \left[\sum_{u \in \mathcal{N}_t(v)} -\log(\sigma(\pi_v^T \pi_u)) \right. \\
& - \sum_{w \in \mathcal{N}_s(v)} \log(\sigma(-\pi_v^T \pi_w)) + I_{label}(v) \cdot JSD(\pi_v || \pi_v^{agent}) \\
& \left. - \mu \sum_{i=1}^N \mathbb{E}_{\mathcal{B}_i^v, \mathcal{B}_i^s} [\log D^{\psi_i}(\{\pi_v\}_{v \in \mathcal{B}_i^v}, \mathcal{B}_i^s)] \right], \tag{11}
\end{aligned}$$

where μ is a positive weight; \mathcal{B}_i^s denotes a set of states obeying the same sampling distribution as that used to train the discriminator; \mathcal{B}_i^v denotes the vertex index set corresponding to \mathcal{B}_i^s .

The complete algorithm of LALA is shown in Algorithm 2.

V. EXPERIMENTS

In this section, we evaluate LALA in multi-agent cooperative navigation task with the same settings used in [7], [8]. In this task, N agents need to cooperate to reach the same number of targets using the minimum time. An example containing three agents and targets is illustrated in Fig. 1.

The task has a continuous state space and a discrete action space. Each agent can observe the relative positions of targets and other agents. At each time step, each agent selects a target and moves a fixed distance (1 m) towards it. Let $a_i \in \{\epsilon\}_{\epsilon=1}^N$ denote the target index selected by an agent. Agents are regarded as mass points. Potential decision conflicts exist in their target selections. Environment size is $15 \times 15 m^2$. Maximum episode length is 30 time steps. Agents are homogeneous. They share a common policy and reward function, which is aligned with [7] and [8]. Reward consists of time penalty $r_{i,step} = -1/L$, conflict penalty $r_{i,conf} = -45/L$, and cooperation award $r_{i,coop} = 0.8/L$, where L is the side length of the environment.

We evaluate the performance of each method in the cases with different numbers of targets and agents ($N = 7, 8, 9$, and 10). In training, agents are trained by 20,000 episodes. At the beginning of each episode, positions of targets and agents are generated randomly. After training, we test the trained policies with 1000 episodes. All experiments are run with three different random seeds.

A. Baselines

We compare the performance of LALA with the following baselines which include a regular MARL algorithm without an advisor, and three algorithms using advisor but with different advising manners. The algorithms using advisor are all implemented based on the regular MARL algorithm and they all use the DualGCN advisor. Detailed descriptions of each baseline algorithm are as follows.

1) *Regular learning without advice (No-Advice)*: We adopt the algorithm proposed in [8] as the baseline method without advising. Each agent takes the positions of targets, the current and last positions of other agents, and its last action as the input of its Q-network. The loss function for the Q-network is given as (3). The Q-network outputs N values that denote the Q-values of N actions. In execution, each agent selects its target according to the maximum Q-values.

2) *Knowledge distillation based advising (KDA)*: We compare LALA with the knowledge distillation [47]–[49] based advising approach where the Q-network with a softmax output layer is regarded as the Student network and the DualGCN used in the advisor learning is regarded as the Teacher network. Instead of leveraging a discriminator to minimize the distribution distance between the policy features of the agent and advisor, KDA directly minimizes the distance between the output of the Student network and the advice given by the Teacher network. We adopt the Jensen-Shannon divergence to measure the distance, and introduce the distance term into the the original loss function of the No-Advice method. The loss for KDA is defined as:

$$\mathcal{L}_{KDA} = \mathcal{L}_\theta + \lambda JSD(\pi^{agent} || \pi^{advisor}), \tag{12}$$

where \mathcal{L}_θ is the loss function of the No-Advice method. π^{agent} is defined as:

$$\pi^{\text{agent}} = \frac{\exp(Q_\theta(s_t, \cdot))}{Z_\theta(s_t)}, \quad (13)$$

where $Z_\theta(s_t)$ is a normalization factor. π^{advisor} is the corresponding advice given by DualGCN.

3) *LALA without advisor boost (LALA-NB)*: To verify the advantage of using advisor boosting method proposed in Section IV-C, we compare LALA with LALA-NB. The loss function for LALA-NB’s advisor is defined as (8). Compared with LALA’s advisor loss (11), LALA-NB does not involve the discriminator’s judgement.

4) *LALA with state-action discriminator (LALA-SA)*: To verify the advantage of PLGAN proposed in Section IV-B, we compare it with a state-action discriminator similar to MAGAIL [13]. The loss function for the discriminator is:

$$\mathcal{L}_{Disc,i}^{\text{LALA-SA}} = -\mathbb{E}_s [\log D^{\psi_i}(s, \pi^{\text{advisor}}) + \log(1 - D^{\psi_i}(s, \pi^{\text{agent}}))], \quad (14)$$

where π^{agent} is the same as (13). The loss function for each agent is defined as:

$$\mathcal{L}_{Agent,i}^{\text{LALA-SA}} = \mathcal{L}_i^{\theta_i} + \lambda \mathbb{E}_s \log(1 - D^{\psi_i}(s, \pi^{\text{agent}})). \quad (15)$$

The advisor’s loss function is defined as:

$$\begin{aligned} \mathcal{L}_{Advisor}^{\text{LALA-SA}} = & \sum_{v \in \mathcal{V}} \left[\sum_{u \in \mathcal{N}_i(v)} -\log(\sigma(\pi_v^T \pi_u)) - \right. \\ & \left. \sum_{w \in \mathcal{N}_s(v)} \log(\sigma(-\pi_v^T \pi_w)) + I_{label}(v) \cdot JSD(\pi_v || \pi_v^{\text{agent}}) \right] \\ & - \mu \sum_{i=1}^N \mathbb{E}_s [\log D^{\psi_i}(s, \pi_v)]. \end{aligned} \quad (16)$$

Compared with the corresponding loss functions for LALA, i.e. (9), (10), and (11), the input of the discriminator is changed from a set of state-action pairs to a single pair of state-action. Note that, unlike MAGAIL, LALA does not require demonstration data. The state data used to represent the advisor and agent is the same, while the action data is different. Therefore, a set of state-action pairs is more appropriate to manifest a policy than a single state-action pair, which suggests that LALA is expected to deliver more scalable and efficient performance than that of LALA-SA.

B. Configurations of LALA

For the MARL agent module, each agent’s decision is defined as (13). The network structure and training configurations are aligned with [8], which is the same as No-Advice. Specifically, the agent module contains a Q-network that has two hidden layers containing 300 and 200 units, respectively. Following [8], an encoder is used to represent the prediction of other agents’ behaviors, which has two hidden layers containing 32 and 16 units, respectively. The replay buffer size is 1500, the batch size of SGD is 32. Adam optimizer with a learning rate of 0.01 is applied to update the parameters.

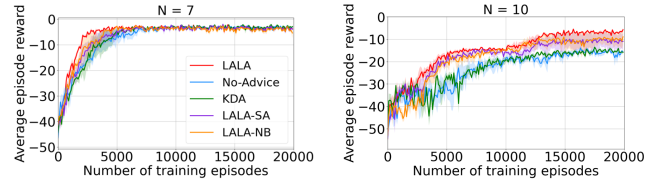


Fig. 4: Convergence curves of average episode reward.

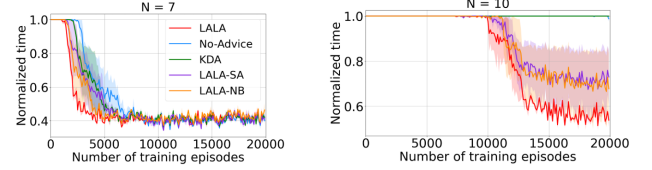


Fig. 5: Convergence curves of normalized navigation time.

In the DualGCN advisor module, we adopt the same structure for the temporal GCN and spatial GCN. Specifically, the temporal/spatial aggregation function in (6) is instantiated with a mean operator. Hidden layers f^k and g^k are fully connected layers with N output units. The activation function ϕ adopts ReLU. The number of hidden layers is set as $K = 2$. Adam optimizer with a learning rate of 0.1 is applied to update the parameters.

For the discriminator, we adopt a three-layer Transformer encoder with four heads, 256 units, and 0.1 dropout rate in each layer. Besides, the input layer projects the raw input as a 64-dimensional vector, and the output layer (classifier) projects the embedding features as a scalar activated by a sigmoid function. Adam optimizer with a learning rate of 0.01 is applied to update the parameters.

C. Macro-Level Performance

1) *Training performance*: Fig. 4 shows the learning curves of the average episode reward of different methods in the cases of $N=7$ and $N=10$. As can be seen from the results, LALA outperforms the other four methods consistently in terms of convergence speed. Additionally, as N increases, LALA can get more average reward than other methods, and especially when $N=10$, the advantage is significant. No-Advice performs the worst in terms of both convergence speed and average reward, as compared with the four methods involving advice. It demonstrates that learning with advice can improve MARL. Fig. 5 shows learning curves of normalized navigation time of different methods. The navigation time refers to the time used by reaching all targets, which equals the time taken by the agent who is the last one to reach a target. If an episode fails, the navigation time is recorded as the maximum episode length. Results in Fig. 5 indicate that LALA converges the most rapidly among all methods.

2) *Execution performance*: We evaluate the execution performance of different methods with two metrics, i.e. cooperation success rate and normalized navigation time. Successful cooperation means that the targets are reached respectively by different agents. Namely, agents can avoid conflicts and

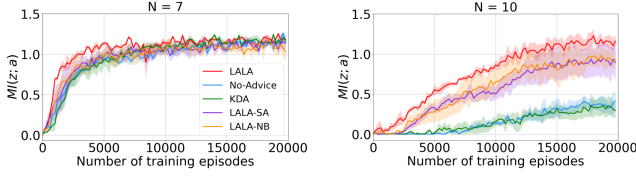


Fig. 6: Curves of mutual information gain.

achieve cooperation. Table I and Table II respectively show the test results of cooperation success rate and normalized navigation time. Each result is recorded with the mean results of three random seeds used in training. As can be seen from the results, LALA achieves the highest success rate and the least navigation time among all methods. Over different N values, LALA performs the most stably in all methods. Notably, the result corresponding to $N=10$ indicates the significant superiority of LALA over other methods.

TABLE I: Cooperation success rate of different methods

	LALA	LALA-NB	LALA-SA	KDA	No-Advice
N=7	0.930	0.890	0.888	0.913	0.874
N=10	0.757	0.520	0.449	0.000	0.015

TABLE II: Normalized navigation time of different methods

	LALA	LALA-NB	LALA-SA	KDA	No-Advice
N=7	0.382	0.408	0.402	0.392	0.414
N=10	0.516	0.667	0.712	1.000	0.990

D. Micro-Level Information Gain

To investigate what happens in agents' decision module at micro level during the process of learning to cooperate, we examine the mutual information between agent's local perceptions and other agents' actions. Specifically, we look into the decision network of an agent, i.e. Fig. 2, and compute the mutual information between the learned representation of other agents' actions and their true actions using the mutual information neural estimator (MINE) [50]. We denote the mutual information as $MI(z; a)$. The curves of the mutual information gain of different methods during training are shown in Fig. 6. As can be seen from the results, $MI(z; a)$ increases as training proceeds. Remarkably, the variation of $MI(z; a)$ is positively correlated with the changes of average episode reward (Fig. 4) in general. Comparing LALA with No-advice, we can see that LALA can enhance $MI(z; a)$ by a large margin. This phenomenon indicates that introducing meso-level coordination to advise micro-level policy learning can enhance agents' mutual understanding about their decisions. Further, the enhancement of agents' mutual understanding promotes the macro-level cooperation performance.

E. Meso-Level Coordination

To investigate the capability of DualGCN regarding meso-level coordination, we examine its cost terms that reflect

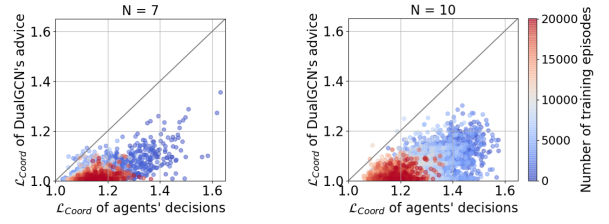


Fig. 7: Coordination loss of agents' decisions and DualGCN's advice.

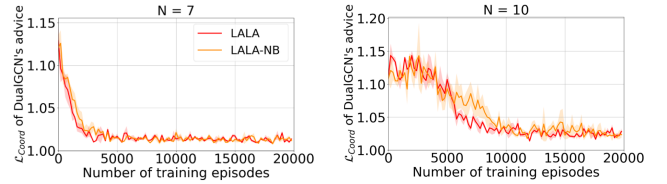


Fig. 8: Convergence curves of DualGCN's coordination loss.

the degree of conflict and temporal discontinuity of agents' decisions. We leverage the cost terms to examine the coordination of both the agents' decisions and the advice given by DualGCN. To be specific, we define a coordination loss based on DualGCN's objective function (11), which is given by:

$$\begin{aligned} \mathcal{L}_{Coord} = & \frac{1}{|\mathcal{V}|} \sum_{v \in \mathcal{V}} \left(\frac{1}{|\mathcal{N}_t(v)|} \sum_{u \in \mathcal{N}_t(v)} -\log(\sigma(\pi_v^T \pi_u)) \right) \\ & - \frac{1}{|\mathcal{N}_s(v)|} \sum_{w \in \mathcal{N}_s(v)} \log(\sigma(-\pi_v^T \pi_w)). \end{aligned} \quad (17)$$

We compute the coordination loss of DualGCN's input (agents' decisions) and output (advice) data in training. Fig. 7 shows the results of cases where $N=7$ and 10 . As can be seen from the results, the coordination loss of DualGCN's advice is lower than that of agents' decisions, which demonstrates the coordination capability of DualGCN. As the number of training episodes increases (from blue to red), the coordination loss of both agents' decisions and DualGCN's advice decreases, which indicates the coordination improvement in both micro-level agents and meso-level DualGCN as training proceeds.

1) *Effect of advisor booster*: To investigate how the advisor booster affects the coordination capability of DualGCN, we compare the convergence curves of the coordination loss of DualGCN trained with LALA and LALA-NB. Results are presented in Fig. 8. Compared with LALA-NB, LALA can promote DualGCN to achieve lower coordination loss during training. It verifies that the advisor booster based on the discriminator's discerning power can further enhance the coordination capability of DualGCN. Besides, for each curve, the convergence point appears earlier than the macro-level average episode reward (Fig. 4). It indicates that meso-level coordination advising causes the improvement of macro-level cooperation performance. Due to the time cost by learning from the advice at micro level, the emergence of macro-level cooperation is delayed.

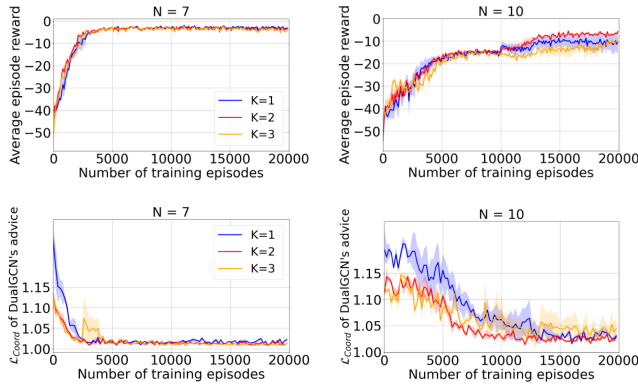


Fig. 9: Performance comparison of different depths of DualGCN. Top row: average episode reward. Bottom row: coordination loss.

2) *Effect of DualGCN's depth*: The depth of DualGCN determines the scope of meso-level coordination of LALA. In the above experiments, the number of hidden layers is $K=2$. In this part, we compare the performance of LALA with $K=1$, 2, and 3. Results are shown in Fig. 9. As can be seen from the bottom row of Fig. 9, $K=1$ results in more coordination loss, which implies the degraded coordination capability. The degraded coordination capability causes less reward, as shown in the top row of Fig. 9. On the other side, when $K=3$, the coordination capability also degenerates. A possible reason is that when K increases, the learned features of each vertex tend to be similar and thus hinder the resolution of conflicts.

VI. CONCLUSION AND FUTURE WORK

We propose LALA approach from the perspective of multilevel emergence dynamics, which leverages the meso-level decision interaction based on agents' spatiotemporal decision structure to advise micro-level decision-making, and thus propels the emergence of macro-level cooperation. LALA involves three-part learning, i.e., DualGCN advisor, agents' decision networks, and advisor-agent discriminators. The DualGCN aggregates agents' decision information and mitigates decision conflicts and discontinuity in spatial and temporal domains, respectively. Agents learn from the coordinated decision advice generated by the DualGCN via PLGAN in addition to their own explorations. The PLGAN includes a discriminator which distinguishes policies of the agent and the advisor, and boosts both of them via its judgement.

By examining the mutual information between agent's local perception and other agents' actions, we reveal that the meso-level coordinated decision advice helps agents' mutual understanding regarding their decisions. Experimental results demonstrate that LALA's advantage in macro-level cooperation performance is positively correlated with its advantage in micro-level mutual information gain and meso-level coordination capability.

Our work elucidated the importance of meso-level coordination for cooperative MARL. We verified our method in a cooperative navigation task. Although it is a representative

and complex multi-agent task, the structure of meso-level coordination is limited relatively. As a future work, we will verify LALA in other tasks to reveal more inspiring results. In addition, the experimental results imply the potential of developing a more powerful GCN and discriminator to promote meso-level coordination, which is worthy of further studies.

REFERENCES

- [1] S. Liu, G. Lever, Z. Wang, J. Merel, S. Eslami, D. Hennes, W. M. Czarnecki, Y. Tassa, S. Omidshafiei, A. Abdolmaleki *et al.*, "From motor control to team play in simulated humanoid football," *arXiv preprint arXiv:2105.12196*, 2021.
- [2] Y. Jin, S. Wei, J. Yuan, and X. Zhang, "Hierarchical and stable multiagent reinforcement learning for cooperative navigation control," *IEEE Transactions on Neural Networks and Learning Systems*, 2021.
- [3] X. Li, J. Zhang, J. Bian, Y. Tong, and T.-Y. Liu, "A cooperative multi-agent reinforcement learning framework for resource balancing in complex logistics network," *arXiv preprint arXiv:1903.00714*, 2019.
- [4] P. Peng, Y. Wen, Y. Yang, Q. Yuan, Z. Tang, H. Long, and J. Wang, "Multiagent bidirectionally-coordinated nets: Emergence of human-level coordination in learning to play starcraft combat games," *arXiv preprint arXiv:1703.10069*, 2017.
- [5] O. Vinyals, I. Babuschkin, W. M. Czarnecki, M. Mathieu, A. Dudzik, J. Chung, D. H. Choi, R. Powell, T. Ewalds, P. Georgiev *et al.*, "Grandmaster level in starcraft ii using multi-agent reinforcement learning," *Nature*, vol. 575, no. 7782, pp. 350–354, 2019.
- [6] Y. Wen, Y. Yang, R. Luo, J. Wang, and W. Pan, "Probabilistic recursive reasoning for multi-agent reinforcement learning," in *International Conference on Learning Representations, ICLR 2019*, 2019.
- [7] Y. Jin, S. Wei, J. Yuan, X. Zhang, and C. Wang, "Stabilizing multi-agent deep reinforcement learning by implicitly estimating other agents' behaviors," in *Proceedings of IEEE International Conference on Acoustics, Speech and Signal Processing*, 2020, pp. 3547–3551.
- [8] Y. Jin, S. Wei, J. Yuan, and X. Zhang, "Information-bottleneck-based behavior representation learning for multi-agent reinforcement learning," in *Proceedings of IEEE International Conference on Autonomous Systems*, 2021.
- [9] P. Sunehag, G. Lever, A. Gruslly, W. M. Czarnecki, V. Zambaldi, M. Jaderberg, M. Lanctot, N. Sonnerat, J. Z. Leibo, K. Tuyls *et al.*, "Value-decomposition networks for cooperative multi-agent learning based on team reward," in *Proceedings of the 17th International Conference on Autonomous Agents and MultiAgent Systems*, 2018, pp. 2085–2087.
- [10] T. Rashid, M. Samvelyan, C. S. D. Witt, G. Farquhar, J. Foerster, and S. Whiteson, "Qmix: Monotonic value function factorisation for deep multi-agent reinforcement learning," in *Proc. Int. Conf. Mach. Learn.*, 2018, pp. 4295–4304.
- [11] K. Son, D. Kim, W. J. Kang, D. E. Hostallero, and Y. Yi, "Qtran: Learning to factorize with transformation for cooperative multi-agent reinforcement learning," in *International Conference on Machine Learning*. PMLR, 2019, pp. 5887–5896.
- [12] N. Jakob, F. Gregory, and A. Triantafyllou, "Counterfactual multi-agent policy gradients," in *The Thirty-Second AAAI Conference on Artificial Intelligence (AAAI 2018)*, New Orleans, 2018.
- [13] J. Song, H. Ren, D. Sadigh, and S. Ermon, "Multi-agent generative adversarial imitation learning," *arXiv preprint arXiv:1807.09936*, 2018.
- [14] L. Yu, J. Song, and S. Ermon, "Multi-agent adversarial inverse reinforcement learning," in *International Conference on Machine Learning*. PMLR, 2019, pp. 7194–7201.
- [15] W. Jeon, P. Barde, D. Nowrouzezahrai, and J. Pineau, "Scalable and sample-efficient multi-agent imitation learning," in *Proceedings of the Workshop on Artificial Intelligence Safety, co-located with 34th AAAI Conference on Artificial Intelligence, SafeAI@ AAAI*, 2020.
- [16] H. M. Le, Y. Yue, P. Carr, and P. Lucey, "Coordinated multi-agent imitation learning," in *International Conference on Machine Learning*. PMLR, 2017, pp. 1995–2003.
- [17] E. Zhan, S. Zheng, Y. Yue, L. Sha, and P. Lucey, "Generative multi-agent behavioral cloning," *arXiv*, 2018.
- [18] S. Sukhbaatar, R. Fergus *et al.*, "Learning multiagent communication with backpropagation," *Advances in neural information processing systems*, vol. 29, 2016.
- [19] J. Foerster, I. A. Assael, N. De Freitas, and S. Whiteson, "Learning to communicate with deep multi-agent reinforcement learning," *Advances in neural information processing systems*, vol. 29, 2016.

- [20] J. Jiang and Z. Lu, "Learning attentional communication for multi-agent cooperation," *Advances in neural information processing systems*, vol. 31, 2018.
- [21] A. Das, T. Gervet, J. Romoff, D. Batra, D. Parikh, M. Rabbat, and J. Pineau, "Tarmac: Targeted multi-agent communication," in *International Conference on Machine Learning*. PMLR, 2019, pp. 1538–1546.
- [22] A. Singh, T. Jain, and S. Sukhbaatar, "Learning when to communicate at scale in multiagent cooperative and competitive tasks," *arXiv preprint arXiv:1812.09755*, 2018.
- [23] S. Li, J. K. Gupta, P. Morales, R. Allen, and M. J. Kochenderfer, "Deep implicit coordination graphs for multi-agent reinforcement learning," in *Proceedings of the 20th International Conference on Autonomous Agents and MultiAgent Systems*, 2021, pp. 764–772.
- [24] J. Ruan, Y. Du, X. Xiong, D. Xing, X. Li, L. Meng, H. Zhang, J. Wang, and B. Xu, "Gcs: Graph-based coordination strategy for multi-agent reinforcement learning." International Conference on Autonomous Agents and Multiagent Systems, 2022, pp. 1128–1136.
- [25] J. Ribeiro, R. Lopes, P. Silva, D. Araújo, D. Barreira, K. Davids, J. Ramos, J. Maia, and J. Garganta, "A multilevel hypernetworks approach to capture meso-level synchronisation processes in football," *Journal of sports sciences*, vol. 38, no. 5, pp. 494–502, 2020.
- [26] S. W. Kozlowski, G. T. Chao, J. A. Grand, M. T. Braun, and G. Kuljanin, "Capturing the multilevel dynamics of emergence: Computational modeling, simulation, and virtual experimentation," *Organizational Psychology Review*, vol. 6, no. 1, pp. 3–33, 2016.
- [27] K. J. Klein and S. W. Kozlowski, "From micro to meso: Critical steps in conceptualizing and conducting multilevel research," *Organizational research methods*, vol. 3, no. 3, pp. 211–236, 2000.
- [28] M. Rogov and C. Rozenblat, "Urban resilience discourse analysis: towards a multi-level approach to cities," *Sustainability*, vol. 10, no. 12, p. 4431, 2018.
- [29] R. Lowe, Y. Wu, A. Tamar, J. Harb, O. P. Abbeel, and I. Mordatch, "Multi-agent actor-critic for mixed cooperative-competitive environments," in *Advances in Neural Information Processing Systems*, 2017, pp. 6379–6390.
- [30] Y. Jin, Y. Zhang, J. Yuan, and X. Zhang, "Efficient multi-agent cooperative navigation in unknown environments with interlaced deep reinforcement learning," in *Proceedings of IEEE International Conference on Acoustics, Speech and Signal Processing*, 2019, pp. 2897–2901.
- [31] L. Liu, Q. Liu, Y. Song, B. Pang, X. Yuan, and Q. Xu, "A collaborative control method of dual-arm robots based on deep reinforcement learning," *Applied Sciences*, vol. 11, no. 4, p. 1816, 2021.
- [32] W. Jacak and K. Pröll, "Conflict resolution in multiagent systems based on wireless sensor networks," in *International Conference on Computer Aided Systems Theory*. Springer, 2009, pp. 753–760.
- [33] W. Jacak and K. Pröll, "Heuristic approach to conflict problem solving in an intelligent multiagent system," in *International Conference on Computer Aided Systems Theory*. Springer, 2007, pp. 772–779.
- [34] N. Tishby and N. Zaslavsky, "Deep learning and the information bottleneck principle," in *IEEE Information Theory Workshop*, 2015, pp. 1–5.
- [35] J. Z. Leibo, V. Zambaldi, M. Lanctot, J. Marecki, and T. Graepel, "Multi-agent reinforcement learning in sequential social dilemmas," in *Proceedings of the 16th Conference on Autonomous Agents and MultiAgent Systems*, 2017, pp. 464–473.
- [36] A. Sanchez-Gonzalez, N. Heess, J. T. Springenberg, J. Merel, M. Riedmiller, R. Hadsell, and P. Battaglia, "Graph networks as learnable physics engines for inference and control," in *International Conference on Machine Learning*. PMLR, 2018, pp. 4470–4479.
- [37] Y. Wu, D. Lian, Y. Xu, L. Wu, and E. Chen, "Graph convolutional networks with markov random field reasoning for social spammer detection," in *Proceedings of the AAAI Conference on Artificial Intelligence*, vol. 34, no. 01, 2020, pp. 1054–1061.
- [38] Y. Li, R. Yu, C. Shahabi, and Y. Liu, "Diffusion convolutional recurrent neural network: Data-driven traffic forecasting," in *International Conference on Learning Representations*, 2018.
- [39] A. M. Fout, "Protein interface prediction using graph convolutional networks," Ph.D. dissertation, Colorado State University, 2017.
- [40] S. Zhang, H. Tong, J. Xu, and R. Maciejewski, "Graph convolutional networks: a comprehensive review," *Computational Social Networks*, vol. 6, no. 1, pp. 1–23, 2019.
- [41] Z. Wu, S. Pan, F. Chen, G. Long, C. Zhang, and S. Y. Philip, "A comprehensive survey on graph neural networks," *IEEE transactions on neural networks and learning systems*, vol. 32, no. 1, pp. 4–24, 2020.
- [42] W. L. Hamilton, R. Ying, and J. Leskovec, "Inductive representation learning on large graphs," in *Proceedings of the 31st International Conference on Neural Information Processing Systems*, 2017, pp. 1025–1035.
- [43] R. Ying, R. He, K. Chen, P. Eksombatchai, W. L. Hamilton, and J. Leskovec, "Graph convolutional neural networks for web-scale recommender systems," in *Proceedings of the 24th ACM SIGKDD International Conference on Knowledge Discovery & Data Mining*, 2018, pp. 974–983.
- [44] M. Zhang, Z. Cui, M. Neumann, and Y. Chen, "An end-to-end deep learning architecture for graph classification," in *Thirty-Second AAAI Conference on Artificial Intelligence*, 2018.
- [45] Y. Jin, Y. Zhang, T. Qin, X. Zhang, J. Yuan, H. Li, and T.-Y. Liu, "Supervised off-policy ranking," *arXiv preprint arXiv:2107.01360*, 2021.
- [46] J. Devlin, M.-W. Chang, K. Lee, and K. Toutanova, "Bert: Pre-training of deep bidirectional transformers for language understanding," in *Proceedings of the 2019 Conference of the North American Chapter of the Association for Computational Linguistics: Human Language Technologies, Volume 1 (Long and Short Papers)*, 2019, pp. 4171–4186.
- [47] G. Hinton, O. Vinyals, and J. Dean, "Distilling the knowledge in a neural network," *arXiv preprint arXiv:1503.02531*, 2015.
- [48] H. Chen, Y. Wang, C. Xu, Z. Yang, C. Liu, B. Shi, C. Xu, C. Xu, and Q. Tian, "Data-free learning of student networks," in *Proceedings of the IEEE/CVF International Conference on Computer Vision*, 2019, pp. 3514–3522.
- [49] I.-J. Liu, J. Peng, and A. Schwing, "Knowledge flow: Improve upon your teachers," in *International Conference on Learning Representations*, 2019.
- [50] M. I. Belghazi, A. Baratin, S. Rajeshwar, S. Ozair, Y. Bengio, A. Courville, and D. Hjelm, "Mutual information neural estimation," in *Proceedings of International Conference on Machine Learning*, 2018, pp. 531–540.